

# Experimental Investigation of Exterior Mechanical Precast Beam Column Connections using Internal Dissipators under Seismic Loading

K. Thulasirajan\* & Revathi.

*Department of Civil Engineering, Pondicherry Engineering College, Puducherry, India.*

\*Email: [kthulasirajan@pec.edu](mailto:kthulasirajan@pec.edu)

**ABSTRACT:** This paper investigates the development and testing of the proposed one-third scaled precast beam column specimens using cleat angle and unbonded threaded rod connection (internal dissipator) under reverse cyclic loading. One monolithic specimen for reference and two precast specimens were studied. The parameters considered in the precast specimens were the presence of stiffener and the action of cement grouting in the predetermined gap of the beam column interface region. The load and displacement were measured for the cyclic loading and thereby strength, hysteretic behaviour, energy dissipation, stiffness, ductility and stiffness degradation were computed and compared. The experimental results showed that the performance of monolithic specimen was superior to precast specimens. The performance of precast specimen with cleat angle and stiffener was found to be superior to precast specimen without stiffener.

**KEYWORDS:** Precast beam column connection, Seismic loading, Cleat angle, Stiffener, Internal dissipator.

## 1 INTRODUCTION

Precast concrete construction plays a vital role in construction industry due to the benefits such as economy, quality and speedy construction. The major task in the design and construction of precast structures are the connection of beam and column elements, especially in seismic prone regions. The precast beam column connections are classified as wet and dry connection based on the presence of cast-in-situ concrete [1-3]. Wet connections are connections in which huge amount of fresh concrete are used at the field to cover the exposed reinforcement in the connection region which emulates the cast-in-situ construction [4]. Dry connections are connections in which external mechanical devices such as cleat angles, tie rods, post tension strands, threaded rods, steel plates etc. are used to connect the precast beam and column members with bolts or welds. Many studies have been conducted on the wet connections and are in field practice. But the demerits of these type of connections are higher reinforcement congestion in the joint core regions, use of extensive formwork and increased construction time and cost. Limited studies have been conducted on dry mechanical connections. Some of the construction details and performance of dry connections reviewed are as follows.

Metelli & Riva (2008) developed a precast beam column dry connection using high strength tensioned steel bars, fibre reinforced concrete grouted in a “Z”

shaped beam column interface and studied for the cyclic behaviour. Although the performance was satisfactory up to 2.5% drift value, pull out of conical fracture radiated from the anchored end of the column was noticed [5]. French et al investigated on seven different type of connection with the plastic hinges determined to form inside and outside the connection regions. It was concluded that the tapered threaded splice connection was found to be the most suitable connection to fabricate and recommended to practice in the moderate to high seismic regions [6, 7]. Vidjeapriya & Jaya (2012) conducted experimental studies on two type of dry connection namely “J” bolt and cleat angle with grouted bolts under reverse cyclic loading. It was revealed that “J” bolt connection was more ductile and energy dissipation as compared to cleat angle connection as the failure occurred at the anchorage region [8]. The load carrying capacity, ductility and energy dissipation capacity were studied for connections using cleat angle with single stiffener and double stiffener. The connection bolts were anchored by grouting and corbel for the support purpose. The performance of cleat angle with double stiffener was superior and recommend to use in low-rise moment resisting frames [9]. Rodriguez & Torres-Matos (2013) verified on the seismic resistance of typical welded reinforcement connection which was currently practiced in urban areas of Mexico. It was concluded that the welded reinforcement connection resulted in brittle failure and unsafe for seismic regions. Further, it was recommended to revise the Mexican building code [10]. Ozden & Ertas (2013) studied on unbounded, post-tension precast

connection with different percentage of mild steel reinforcement. It was revealed that the hybrid connection showed small or negligible damage to beam and column member and the authors suggested to use 20 to 30% of mild steel for adequate strength, ductility, energy dissipation and residual strength [11].

The present study investigates on the development of proposed precast beam column connection for seismic prone regions using cleat angle and unbonded threaded rods for connecting the beam and column members. The major advantage of this type of connections are the easily replaceable unbonded threaded rods after the occurrence of an earthquake event and act as an internal dissipator. Moreover the presence of grouted dowel bar hold the beam member after the failure of the unbonded internal dissipators. Further the presence of corbel facilitates easier and faster installation of the connection. The proposed system of precast beam column connection along with the internal dissipators is shown in Figure 1.

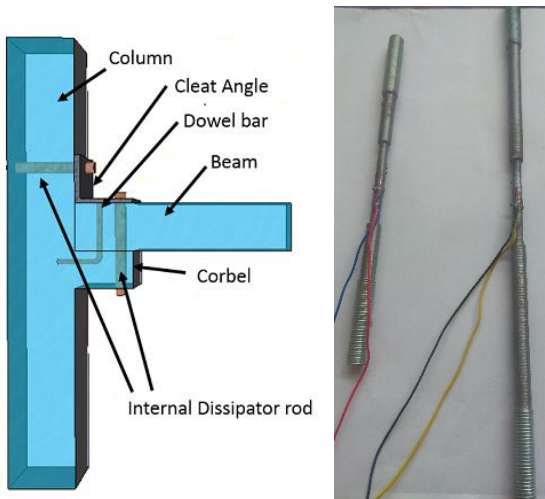


Figure 1 - Proposed beam column connection and internal

## 2 EXPERIMENTAL INVESTIGATION

### 2.1 Materials characteristics

Beam column specimens were cast with concrete whose compressive strength determined from the compression test at 28 days was 45.2 MPa. The modulus of the elasticity of the concrete obtained was 27.29 GPa. 8 mm and 4 mm diameter rods were used as reinforcements. The ultimate tensile strength of the 8 mm diameter deformed main reinforcement and 4 mm diameter stirrups were found to be 670 MPa and 700 MPa respectively. Similarly, the ultimate tensile strength of the internal dissipator was found to be 630 MPa. Cement grout with an average mortar strength

of 25 MPa was used as the filler material in the precast beam column interface region and in dowel bar region.

### 2.2 Description of specimens

Exterior beam column connection of a three storey building with each storey height of 3.5 m and 3 m length between the columns were analyzed for the lateral forces as per IS: 1893 (2002) [12] and designed based on the guidelines given in IS: 456 (2000) [13] and IS 13920 (1993) [14]. The test specimens were scaled down to one-third prototypes using similitude law [15] and the details of the prototype are presented in Table 1.

Table 1 – Details of the monolithic specimen

Details	Specifications
Beam dimension (mm)	600 x 120 x 100
Beam main bars	4 nos of 8 mm $\Phi$ bars
Beam stirrups	2 legged 4 mm $\Phi$ bars @ 30 mm spacing for a distance of 220 mm and beyond 220mm the spacing of stirrups were 60 mm
Column dimension (mm)	1400 x 120 x 100
Column main bars	4 nos of 8 mm $\Phi$ bars
Column stirrups	2 legged 10 mm $\Phi$ bars @ 25 mm spacing for a distance of 180 mm and beyond 180 mm the spacing of stirrups were 50 mm

The monolithic specimen is designated as ML. The reinforcement details of monolithic and precast specimens are shown in Figure 2. Similar reinforcement details were followed in the precast specimens. Additionally, precast beam element was reinforced with two numbers of 4 mm diameter horizontal stirrups spaced at a distance 33 mm from the beam top face. The size of the corbel was 120 x 120 x 100 mm. The corbel was reinforced with two number of 8 mm diameter vertical reinforcement along the sides and one number of 8 mm diameter “U” shaped horizontal reinforcement. In addition, two number of 2 legged 4 mm diameter vertical stirrups spaced at 40 mm from the column face and one number of 2 legged 4 mm diameter horizontal stirrup was placed at the mid height of the corbel section. The ISA 100 x 100 x 10 mm cleat angle was used with 14 mm diameter holes drilled in the vertical and horizontal legs. The holes were drilled at a distance of 75 mm from the inner face of the cleat angle. Two sleeve holes were formed at a distance of 35 mm and 75 mm from the beam end region for the insertion of the 6 mm dowel bar and internal dissipator respectively. Sleeve hole was formed in the corbel at a distance of 80 mm from the

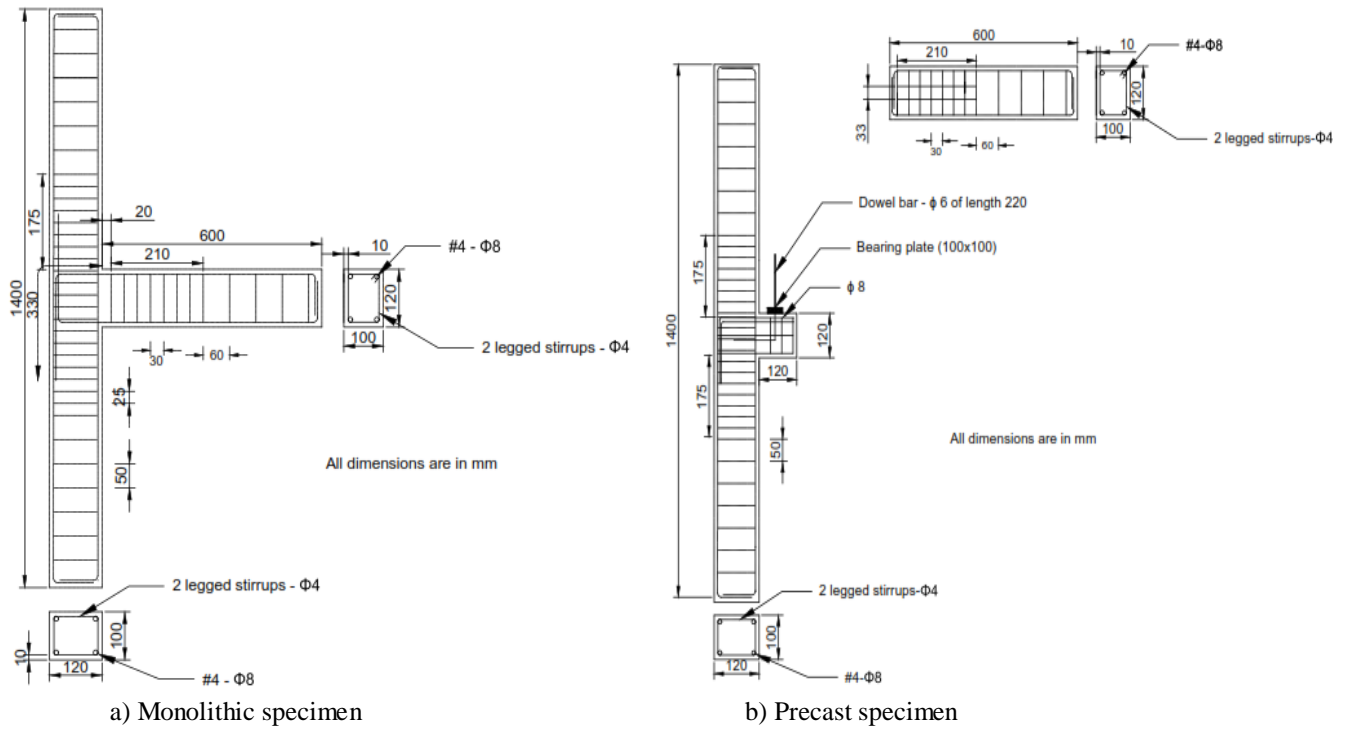


Figure 2 - Reinforcement details

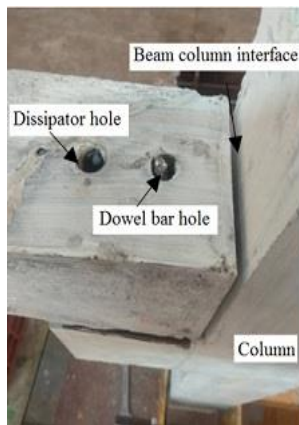


Figure 3 - Pictures of PBC-NS specimen

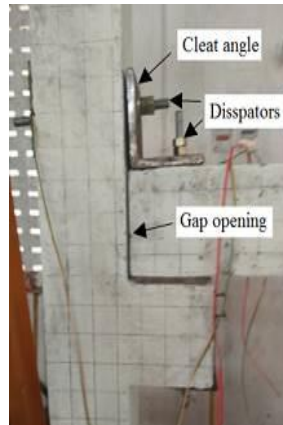


Figure 4 - Pictures of PBC-SS specimen

column face to provide 5 mm tolerance for the beam fixation. Similarly, the vertical leg of the cleat angle was connected with dissipators to the column region by the sleeve hole which was formed in the column at a distance of 200 mm. The yield length of 60 mm with a diameter of 6 mm were provided to the middle region of the dissipators.

The first precast specimen was connected by cleat angle with no stiffener and was not grouted in-between the beam column interface region. This specimen is designed as PBC-NS. The second precast specimen was connected by cleat angle with stiffener and grouted in-between the beam column interface region. This specimen is designated as PBC-SS. The stiffener used was of size 40 x 40 x 10 mm. Cement



grout was used to grout the gaps in the beam dowel bar hole and gap in-between the beam column interface. Steel bearing plate of size 100 x 100 x 6 mm was used in-between the corbel and beam member. The pictures of PBC-NS and PBC-SS are shown in Figures 3-4.

### 2.3 Precast connection assembly

Initially, column was fixed in the loading frame. Then the bearing steel plate was placed in the corbel with the dowel bar protruding from the corbel. The beam was placed with the dowel bar inserted in the beam dowel bar hole as shown in the Figure 3. Alignment was made to fix the internal dissipators in the beam corbel region and the column region. Cement grouting was done in the beam dowel bar hole. Further the cleat angle was placed and the internal dissipators were fixed with nuts and washers.

### 2.4 Test setup and loading protocol

The test setup consist of a loading frame of 50 kN capacity. A push-pull hydraulic jack of 30 kN capacity was used for the application of cyclic loading and controlled by hydraulic power pack machine. A 10 % constant axial load of column strength [9, 16, 17] was applied on the column top using 500 kN hydraulic jack, to induce the dead load transfer from the upper floor. The top and bottom ends of the column were fixed. Displacement controlled reverse cyclic loading system was followed. The drift ratio is defined as the ratio of beam end displacement to the beam length. The beam end displacement was measured using two linear variable differential transducer (LVDTs) which was placed at the top and bottom of the beam member. A tension-compression type load cell of 100 kN capacity was attached to the push pull hydraulic jack to measure the applied load. Data logger was used to acquire the data from the load cell and the LVDTs. The experimental setup and the cyclic loading history are shown in Figures 5-6.

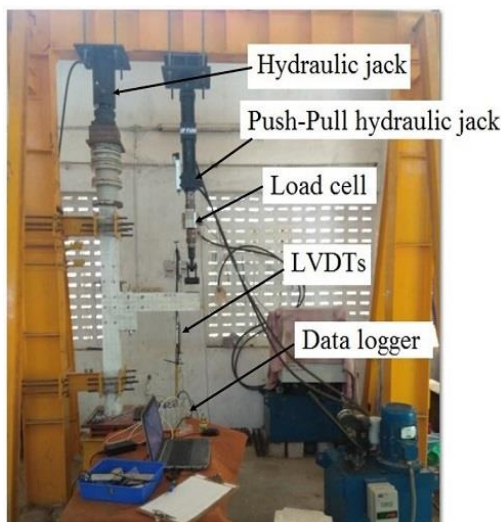


Figure 5 - Experimental setup

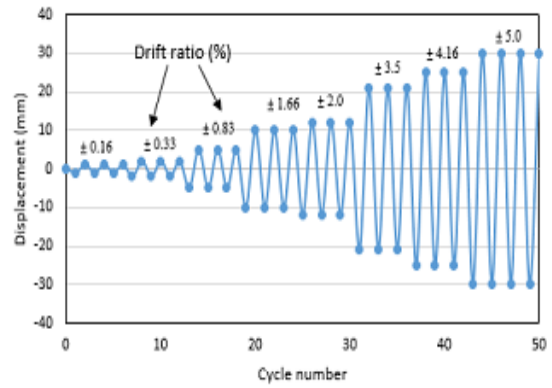


Figure 6 - Loading protocol

## 3 RESULTS

### 3.1 Mode of failure

The failure mode of the specimens at 10 mm and 25 mm displacement cycles are shown in Figures 7-9. In the ML specimen, flexural cracks initiated at beam column interface and in the beam region corresponding to 2 mm displacement cycle. Diagonal shear cracks occurred in the joint core region at 10 mm displacement cycle. With further increase in the displacement cycle, resulted in the concentrated crack widening at beam column interface and at a distance of 45 mm from the column face. For the specimen PBC-NS, localized cracks initiated at the corner of the beam region corresponding to 2 mm displacement cycle, which was near to column face. Flexural crack occurred at anchorage region of internal dissipator corresponding to 10 mm displacement cycle. But at 12 mm displacement cycle, shear crack also continued from the same location joining the flexural crack. With further increase in the displacement cycles resulted in the crushing and spalling of concrete at the beam end which was nearer to the column face. The specimen PBC-SS also exhibited similar crack formation as of PBC-NS, but the crack initiated at 1 mm displacement cycle. Further the crack width measured at 10 mm displacement cycle was found to be 5 mm. Additionally, at 21 mm displacement cycle, flexural crack occurred at the anchorage location of the internal dissipator and propagated as shear crack to the core region of the beam. Flexural crack was also observed at a distance of 160 mm from the column face. In all the precast specimens, localized failure was observed in beam region but no damage was observed in the column region indicating strong column and weak beam condition.

### 3.2 Strength

The ultimate strength of the ML specimen in the positive and negative loading directions were about 10.3 kN and 10.01 kN respectively. For the specimen PBC-NS, the ultimate strength in the positive and

negative loading directions were found to be 7.20 kN and 1.5 kN respectively. Similarly, for the specimen PBC-SS, the ultimate strength in the positive and negative loading directions were found to be 7.44 kN and 3.66 kN respectively. Overall, the ultimate strength of ML specimen in both the loading directions were superior to the precast specimens. The ultimate strength of precast specimens in the positive and negative loading direction are dissimilar due to the presence of corbel. The presence of corbel results in higher

strength resistance in the positive loading direction as compared to negative loading direction. The strength of PBC-SS specimen in the negative loading direction was higher to PBC-NS specimen which is attributed to the presence of stiffener and grouting of the predefined gap opening in the beam column interface, thereby negative forces are transferred and resisted by the dissipators. Figure 10 shows the strength comparison of the specimens



a) at 10 mm displacement cycle



b) at 25 mm displacement cycle

Figure 7 - Failure mode of ML specimen



a) at 10 mm displacement cycle



b) at 25 mm displacement cycle

Figure 8 - Failure mode of PBC-NS specimen



a) at 10 mm displacement cycle



b) at 25 mm displacement cycle

Figure 9 - Failure mode of PBC-SS specimen

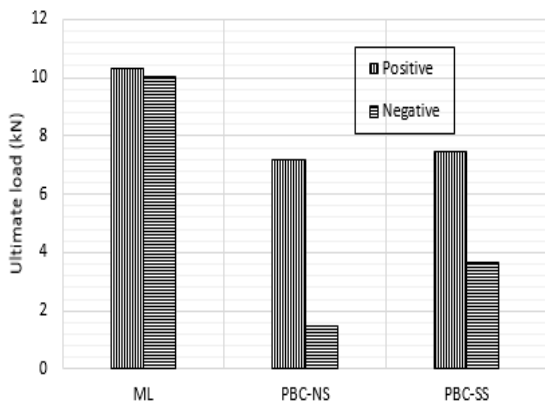


Figure 10 - Strength comparison of the specimens

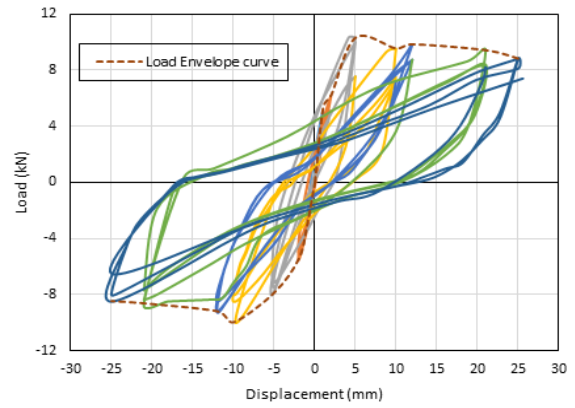


Figure 11 - Hysteretic behaviour of ML specimen

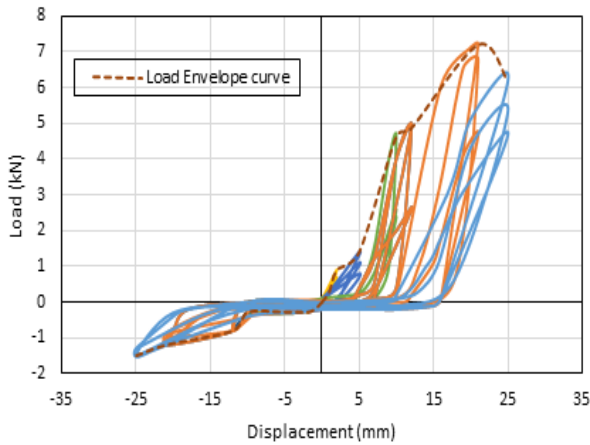


Figure 12 - Hysteretic behaviour of PBC-NS specimen

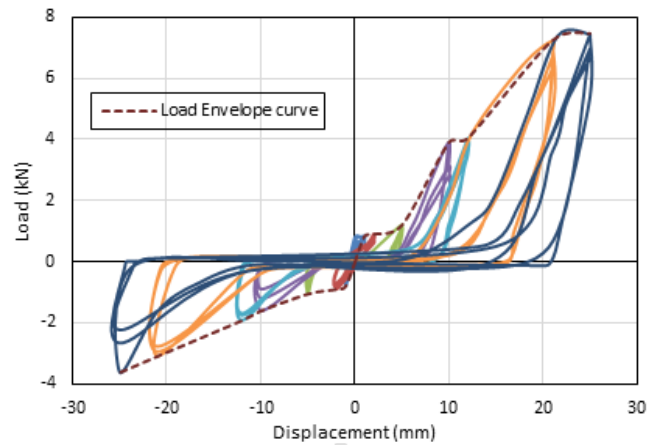


Figure 13 - Hysteretic behaviour of PBC-SS specimen

### 3.3 Hysteretic behavior

The load displacement hysteresis loops for the specimens are presented in Figures 11-13. The hysteresis loop pattern of ML specimen was almost similar in both the loading direction. Slight pinching effect was observed from the 10 mm displacement cycle which was due to formation of diagonal crack in the joint core region. The diagonal crack was due to the bond failure of the embedded beam main reinforcement. Greater pinching effect was noticed in the precast specimens which may be attributed to the presence of predefined gap opening in the beam column interface region.

### 3.4 Stiffness and ductility

Figure 14 shows the definition of the secant stiffness ( $K_{sec}$ ) which was calculated based on the slope of the idealized load envelope curve considering the 75 % of the ultimate load ( $P_u$ ) and the corresponding displacement ( $\Delta_e$ ) [16,18]. Table 2 present the secant stiffness of the specimens. The secant stiffness for ML specimen was found to be 2.24 kN/mm. The PBC-SS specimen (0.24 kN/mm) had slight increase in secant stiffness as compared to PBC-NS specimen (0.21 kN/mm). Overall, the precast specimen offered

very low secant stiffness as compared to ML specimen.

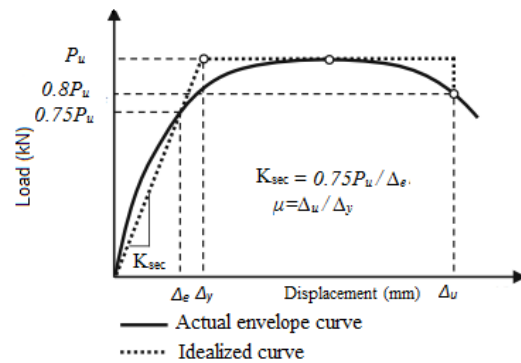


Figure 14 - Definition for secant stiffness and ductility [18]

### 3.5 Energy Dissipation

The cumulative energy dissipation for the specimens were obtained by summing the energy dissipated for every displacement cycles and shown in Figure 15. The energy dissipated by ML, PBC-NS and PBC-SS specimens were found to be 1717.5 kN-mm, 253.9 kN-mm and 410.1 kN-mm respectively. It was observed that the ML specimen dissipates more energy with the interaction of the exposed beam main reinforcement rods beyond the 10 mm displacement cycle. Further, the PBC-SS specimen exhibited slight increase in energy dissipation as compared to PBC-NS specimen which is due to the presence of stiffener



and grouted material which transferred the cyclic (upto 10 mm). Hence, for comparison, the stiffness

Specimen	Loading direction	Yield load $P_y$ (kN)	Displacement corresponds to yield load $\Delta_e$ (mm)	Secant stiffness $K_{sec}$ (kN/mm)	Average secant stiffness (kN/mm)
ML	Positive	7.72	2.8	2.74	2.24
	Negative	7.5	4.3	1.74	
PBC-NS	Positive	5.41	14.1	0.38	0.21
	Negative	1.12	23	0.04	
PBC-SS	Positive	5.58	16.1	0.35	0.24
	Negative	2.7	18.8	0.14	

loads to the dissipator rod.

### 3.6 Stiffness degradation

The stiffness degradation was presented based on the first cycle of each set of displacement cycle and determined based on the peak to peak stiffness method [16]. The stiffness degradation for all the specimens are shown in Figure 16. The initial stiffness of ML specimen was higher followed by PBC-SS and PBC-NS specimens. The stiffness degradation of ML specimen was faster in the initial displacement cycles

was normalized ( $K_{norm}$ ) with respect to the stiffness measured at 10 mm displacement cycle and presented in the Figure 17. The loss in the stiffness of ML, PBC-NS and PBC-SS specimens at 25 mm displacement level were found to be 64.5 %, 37.51 % and 19.63 % respectively. The loss in the stiffness of the ML specimen is due to the opening and closing of cracks, concrete crushing and bond degradation. For the precast specimens, the loss in the stiffness were comparatively lesser to ML specimen with minor interaction of the internal dissipator.

Table 2 – Secant stiffness of the specimens

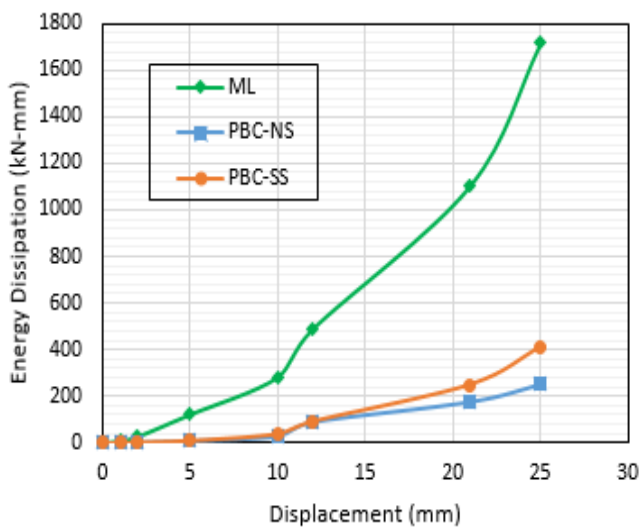


Figure 15 - Energy dissipation of the specimens

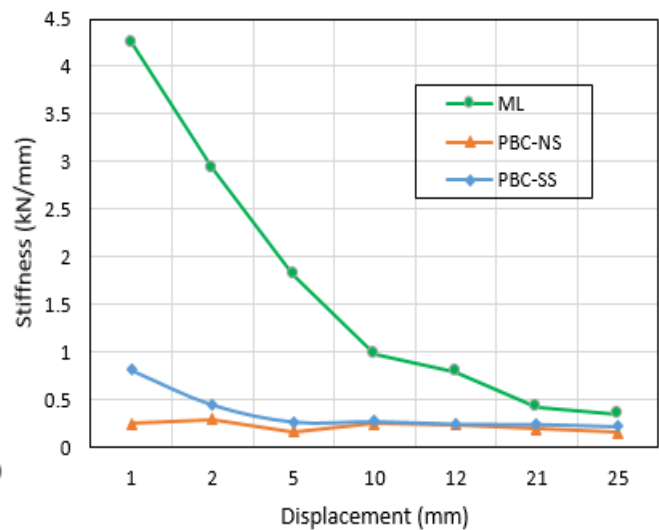


Figure 16 - Stiffness degradation of the specimens

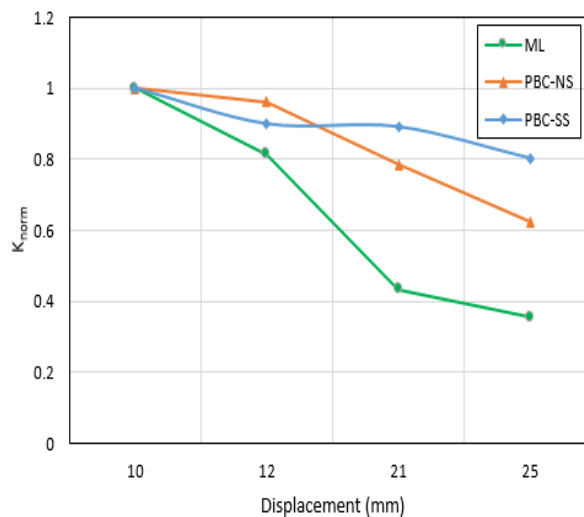


Figure 17 - Normalized stiffness degradation of the specimens

#### 4 CONCLUDING REMARKS

Based on the test results and observation made on the exterior monolithic and precast beam column connections, the following conclusion are drawn:

- The performance of ML specimen was superior to precast specimens in terms of strength, hysteretic behaviour, energy dissipation and stiffness.
- The presence of corbel in the precast specimens resulted in increased strength resistance in the positive loading direction.
- The pinching effect was greater in precast specimens due the failure of the concrete edges near the beam end of the column face.
- The strength and energy dissipation in the negative loading direction of PBC-NS specimen was comparatively lower to PBC-SS specimen. This is due to the presence of stiffener and grouted predefined gap opening in the beam column interface, which made the negative forces to transfer and resisted by the internal dissipators.
- The stiffness of both the precast specimens were inferior to ML specimen which is due the formation of localized crushing and cracking failure in the precast beam region.
- The loss in the initial stiffness of precast specimens was lower as compared to ML specimen. Thus indicating minimal cyclic force transferred to the dissipator rod.
- In all the precast specimens, localized failure was observed in the beam element, with no damage observed in the column region demonstrating strong column and weak beam condition.

Even though, the performance of PBC-SS specimen was better than PBC-NS specimen, modification to the existing precast connection system need to be done to improve the strength, energy dissipation and

stiffness characteristics. Moreover, the crack formation and crushing of the concrete in the beam end nearer to the column face has to be prevented and action of dissipators are to be created with minimum or less damage to the beam region. Thereby, the dissipators can be replaceable after the occurrence of an earthquake event.

#### ACKNOWLEDGMENTS

This work was supported by University Grant Commission (UGC-MRP), India which was a sponsored project on “Recycled Aggregate Geo-Polymer Concrete for Pre-cast Reinforced Concrete Elements”. The authors whole heartily wish to gratitude for the financial support.

#### REFERENCES

1. Stanton J.F., Hawkins N.M., Hicks T.R., PRESSS project 1.3: connection classification and evaluation. PCI Journal, vol. 36, issue 5, 1991, pp. 62-71.
2. ACI 550.2R-13, Design Guide for Connections in Precast Jointed Systems, Joint ACI-ASCE Committee 550, Farmington Hills, MI, USA, 2013.
3. Pul S., Senturk M., A bolted moment connection model for precast column-beam Joint. In the Proceedings of the 2<sup>nd</sup> World Congress on Civil, Structural, and Environmental Engineering, Barcelona, Spain, April 2017.
4. Joshi M.K., Murty C.V.R., Jaisingh, M.P., Cyclic behaviour of precast RC connections. Indian Concrete Journal, November 2005, pp 43-50.
5. Metelli G., Riva P., Behaviour of a beam to column “Dry” jointed for precast concrete elements. In the 14<sup>th</sup> World Conference on Earthquake Engineering, Beijing, China, January 2008.
6. French C.W., Amu O., Tarzikhian C., Connection between precast elements - failure outside connection region. Journal of Structural Engineering- ASCE, vol. 115, issue 2, 1989, pp. 316-340.
7. French C. W., Hafner M., Jayashankar, V., Connections between precast elements - Failure within connection region.



- Journal of Structural Engineering- ASCE, vol. 115, issue 12, 1989, pp. 1371-1391.
8. Vidjeapriya R., Jaya, K.P., Behaviour of precast beam-column mechanical connections under cyclic loading. *Asian Journal of Civil Engineering (Building and Housing)*, vol. 13, issue 2, 2012, pp. 233-245.
  9. Vidjeapriya R., Jaya K.P., Experimental study on two simple mechanical precast beam-column connections under reverse cyclic loading. *Journal of Performance of Constructed Facilities*, vol. 27, issue 4, 2013, pp. 402-414.
  10. Rodriguez M.E., Torres-Matos M., Seismic behavior of a type of welded precast concrete beam-column connection. *PCI Journal*, vol. 58, issue 3, 2013, pp. 81-94.
  11. Ozden S., Ertas O., Behavior of unbonded, post-tensioned, precast concrete connections with different percentages of mild steel reinforcement. *PCI Journal*, vol. 52, issue 2, 2007, pp. 32-44.
  12. IS: 1893 (2002), Code of practice for criteria for earthquake resistant design of structures: Part- 1 General provisions and buildings, Bureau of Indian Standards, New Delhi, India.
  13. IS: 456 (2000), Indian standard code of practice for plain and reinforced concrete, Bureau of Indian Standards, New Delhi, India.
  14. IS: 13920 (1993), Code of practice for ductile detailing of reinforced concrete structures subjected to seismic forces, Bureau of Indian Standards, New Delhi, India.
  15. Vidjeapriya R., Behaviour of precast beam-column connections subjected to seismic type loading. Ph.D. thesis, Anna University, Chennai, December 2011.
  16. Saqan E.I., Evaluation of ductile beam column connections for use in seismic resistant precast frames. Ph.D. thesis, University of Texas, Austin, December 1995.
  17. Cheok G.S., Lew H.S., Model precast concrete beam-to column connections subjected to cyclic loading. *PCI Journal*, vol. 38, issue 4, 1993, pp. 80-92.
  18. Truong G.T., Dinh N.H., Kim J., Choi, K., Seismic performance of exterior RC beam-column joints retrofitted using various retrofit solutions. *International Journal of Concrete Structures and Materials*, vol. 11, issue 3, 2017, pp. 415-433.